

## ELECTRICAL AND THERMAL MODELING OF RAILGUNS

Jerry F. Kerrisk  
Los Alamos National Laboratory  
P. O. Box 1663  
Los Alamos, NM 87545

Summary

Electrical and thermal modeling of railguns at Los Alamos has been done for two purposes: (1) to obtain detailed information about the behavior of specific railgun components such as the rails, and (2) to predict overall performance of railgun tests. Detailed electrical and thermal modeling has concentrated on calculations of the inductance and surface current distribution of long parallel conductors in the high-frequency limit and on calculations of current and thermal diffusion in rails. Inductance calculations for various rail cross sections and for magnetic flux compression generators (MFCG) have been done. Inductance and current distribution results were compared with experimental measurements. Two-dimensional calculations of current and thermal diffusion in rail cross sections have been done; predictions of rail heating and melting as a function of rail size and total current have been made. An overall performance model of a railgun and power supply has been developed and used to design tests at Los Alamos. The lumped-parameter circuit model uses results from the detailed inductance and current diffusion calculations along with other circuit component models to predict rail current and projectile acceleration, velocity, and position as a function of time.

Inductance and Current Distribution

A method has been developed to calculate current-density distribution, magnetic field, and inductance of railgun conductors, or other long, parallel conductors of arbitrary cross section, in the high-frequency limit.<sup>1</sup> In this limit, all current flow occurs on the conductor surfaces. The current-distribution problem is equivalent to the calculation of charge distribution on equipotential (electrostatic) surfaces. For conductors that are long in the  $z$ -direction, the  $z$ -component of the magnetic vector potential is equivalent to the electrostatic potential. Only the  $z$ -component of the current density and the  $x$ - and  $y$ -components of the magnetic field are nonzero. The proper current-density distribution is that which produces a constant value of the magnetic vector potential on each conductor surface. The current distribution is approximated by a sequence of cubic splines that minimizes the error in the vector potential on the conductor surfaces in the least-squares sense. Values of the vector potential on conductor surfaces represent boundary conditions for this calculation. They are determined from total current flow in the circuit and geometric symmetry of the conductors. Once the current distribution is known, the magnetic field outside the conductors can be calculated from the definition of the magnetic vector potential. In particular, the total flux that links the circuit can be determined from the field between the conductors. The self inductance of the rails is easily calculated from the flux linkage. One theoretical limitation of this method is that conductor surfaces cannot have square corners; the corner region must be replaced by a circular arc of the appropriate radius. This has not proved to be a practical limitation.

Calculated current distributions and inductances have been compared with other theoretical calculations and with measured data.<sup>1</sup> For two long, parallel conductors of circular cross section, the calculated current distribution and inductance were in excellent agreement with theoretical values. Measurements of the inductance of two rectangular conductors and of two rectangular conductors in a tube have been reported as a function of frequency. Calculated values of the inductance for these circuits are generally in good agreement with the highest frequency measurements. Calculations of the current distribution on thin rectangular conductors also compared well with measurements made in an electrolytic tank.

Figure 1 shows a plot of a conductor cross section in the first quadrant (solid line) and magnetic-field lines (dotted lines) for two rectangular conductors that are 4 mm high by 2 mm wide with a 6 mm separation. Because the geometry is symmetric about the  $x$  and  $y$  axes, only the first quadrant is shown. Figure 2 shows a plot of the surface current density as a function of arc length along the conductor surface; the zero of arc length is at the point (5,0), on the outside surface of the conductor. The peaks represent current density in the vicinity of the corners. The current density on the inner surface is greater than on the top or outer surface. The magnitude of the difference is a function of conductor shape and separation. Inductance calculations for two rectangular conductors have been fitted to an empirical equation in the height ( $H$ ), width ( $W$ ), and separation ( $S$ ). Figure 3 shows a plot of calculated inductance plotted as a function of  $S/H$  for various values of  $W/H$ . Similar calculations and correlations have been made for other conductor

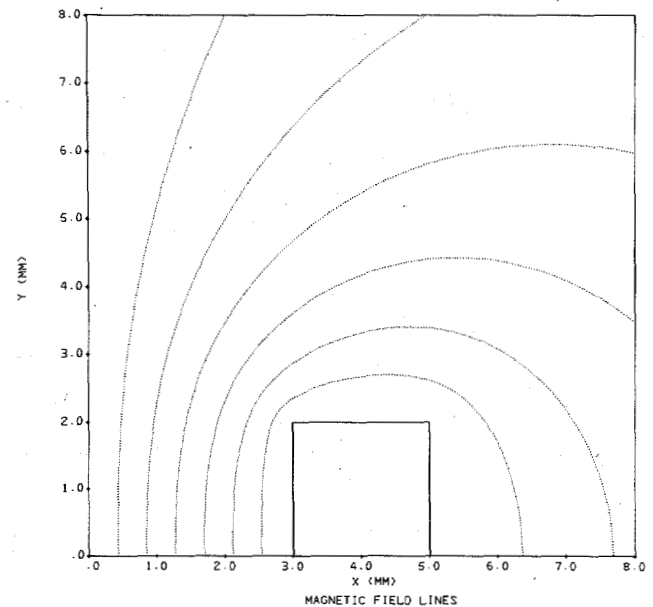


Fig. 1. Conductor cross section (solid lines) and magnetic field (dotted lines) for two rectangular conductors.

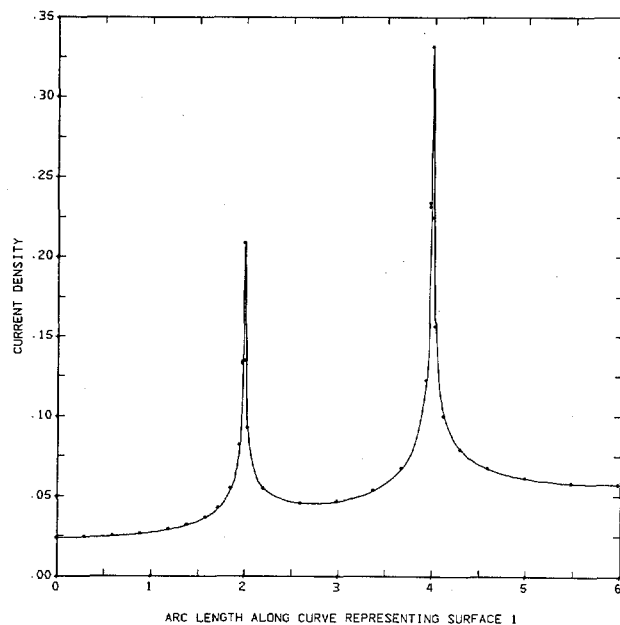


Fig. 2. Relative current density as a function of arc length in mm for two rectangular conductors.

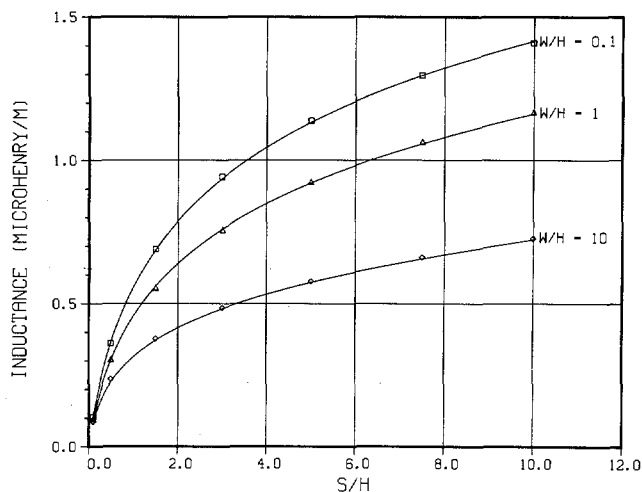


Fig. 3. Inductance of two rectangular conductors as a function of  $S/H$ .

cross-sectional shapes, for conductors inside a metallic tube, and for MFCG conductors.

#### Current and Thermal Diffusion

At any axial location along the rails, current will start to flow in the rail cross section as the projectile passes. For rails with their cross section in the  $x$ - $y$  plane, only the  $z$ -component of the current density and the  $x$ - and  $y$ -components of the magnetic field are nonzero. Initially, current is distributed over a thin layer near the surface of each conductor. The current density is not uniform on the surface; it is a function of the shape and separation of the conductors as shown in the previous section. With time, the current and associated magnetic field diffuse into the conductors. Because large current densities are involved, local heating occurs in the rails. This changes rail properties such as electrical conductivity. Thus, the current-diffusion process is nonlinear. In addition, thermal diffusion

is occurring simultaneously with current diffusion. The thermal-diffusion process is also nonlinear. The time scale over which current diffusion occurs is so short that thermal diffusion is normally neglected.

Most analyses of these phenomena have dealt with one-dimensional magnetic-field diffusion in flux-compression generators. For railgun conductors, a two-dimensional calculation is required, and current, not magnetic-field strength, is the primary variable. In the linear case, magnetic-field strength and current density obey the same partial differential equation, the linear thermal diffusion equation. This is not true in the nonlinear case. In a two-dimensional, nonlinear calculation, coupled partial-differential equations for the components of a vector quantity such as the magnetic-field strength may be required. Thus, the geometry of a problem and the quantities known as initial and boundary conditions play a very important part in the complexity of the solution.

Starting from Maxwell's equations, a diffusion-like equation for the magnetic-field strength ( $H$ ) can be obtained,

$$-\nabla^2 H + \mu \sigma (\partial H / \partial t) = (1/\sigma) [\nabla \sigma \times (\nabla \times H)] ,$$

where  $\sigma$  is the electrical conductivity,  $\mu$  is the magnetic permeability, and  $t$  is time. For a railgun conductor, two coupled partial differential equations in the  $x$ - and  $y$ -components of  $H$  result. A similar equation in terms of the electric field strength ( $E$ ) can be obtained,

$$-\nabla^2 E + \mu \sigma (\partial E / \partial t) = -\mu E (\partial \sigma / \partial t) .$$

For railgun conductors, a single partial differential equation in the  $z$ -component of  $E$  or the current density ( $j = \sigma E$ ) can be written. This equation can be solved as a nonlinear thermal-diffusion problem if  $-\mu E (\partial \sigma / \partial t)$  is treated as a source term.

A formulation of this problem in terms of current density has been applied by adapting a finite-difference, heat-transfer computer program to the simultaneous calculation of current and thermal diffusion.<sup>2</sup> A series of test calculations of current density and rail temperature has been made for various rectangular rails. The geometry of the conductors is symmetric about the  $x$  and  $y$  axis. Thus, it is only necessary to model half of one conductor, the portion in the first quadrant. Figure 4 shows a schematic of one of the 10 x 10 rectangular meshes with variable spacing used for these calculations; a few node numbers are shown. The total current is assumed known as a function of time. Changes in total current are made by changing current density in the edge nodes only; that is, it is assumed that current density or electric field strength enters or leaves the conductor through its exterior surfaces. Surface current distributions described in the previous section are used to distribute current to the surface nodes of the conductor. Figures 5 and 6 show the variation of current density in nodes 201 (an edge node near the corner) and 1005 (an internal node) as a function of time for a 10-mm-high by 10-mm-wide rail with 0.66 MA constant current. Note the large differences in maximum current density and variation with time. Node temperatures are a function of Joule heating in each node and heat gains and losses to surrounding nodes and the environment. In this calculation, temperatures of surface nodes near the two corners were above the melting point. Two electrical parameters, the resistance and inductance per unit length of rails, can also be determined

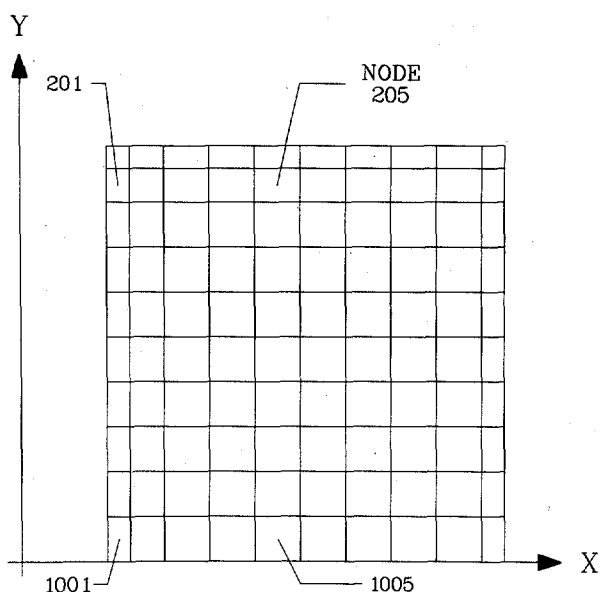


Fig. 4. 10 x 10 rectangular mesh on half of one rail.

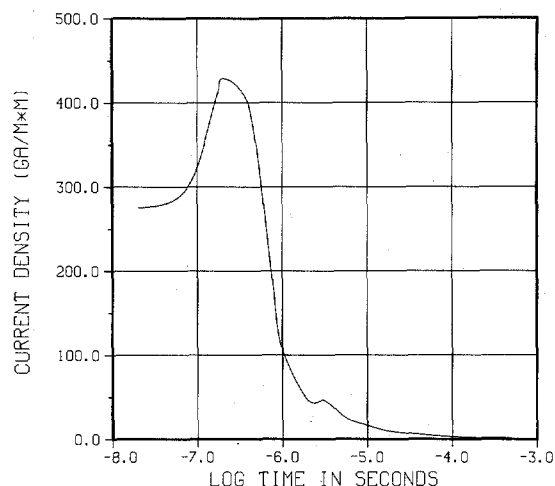


Fig. 5. Node 201 current density as a function of time for 10-mm by 10-mm rail.

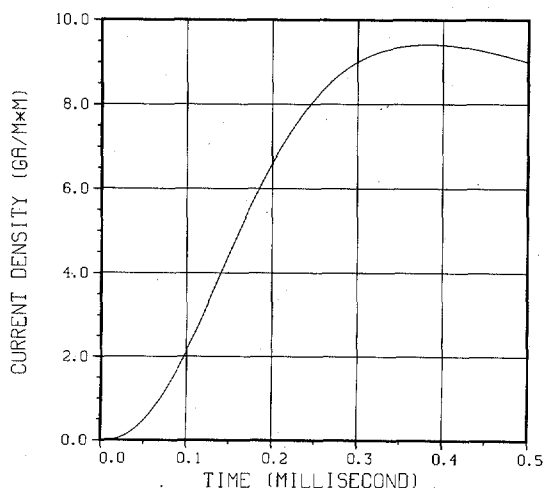


Fig. 6. Node 1005 current density as a function of time for a 10-mm by 10-mm rail.

during these calculations; these results were used to formulate models for the performance calculations described in the next section.

### Performance Model

A lumped-parameter circuit model for predicting the performance of railgun tests from a description of the power supply and railgun has been developed and used to design tests and analyze test results. The model combines a calculation of the electrical behavior of the railgun circuit with a calculation of projectile acceleration, velocity, and position. The present version includes a primary power supply (capacitor bank), a strip generator (MFCG),<sup>3</sup> and a railgun load (see Fig. 7). It can accommodate more than one MFCG in the circuit, fired simultaneously or sequentially. The analysis is complicated by the significant variation of the inductance of the generator ( $L_G$ ) and the railgun ( $L_L$ ) during a test;  $L_G$  decreases with time as the generator burns and  $L_L$  increases as the projectile moves, bringing more rails into the circuit. The differential equation for the circuit,

$$\frac{d(LI)}{dt} + RI + \frac{1}{C} \int_0^t I dt = V,$$

is solved numerically using Euler's method. In this equation,  $t$  is time,  $I$  is current,  $L$  is total inductance,  $R$  is total resistance,  $C$  is bank capacitance, and  $V$  is the voltage (capacitor voltage plus other miscellaneous voltages). At each time step, projectile acceleration is calculated as

$$\frac{d^2x}{dt^2} = \frac{L_{HF} I^2}{2m} - \frac{F_f}{m},$$

where  $L_{HF}$  is the high-frequency-limit inductance per unit length of the rails,  $m$  is projectile mass,  $x$  is projectile position, and  $F_f$  is the retarding (friction) force on the projectile.

For a test, the capacitor bank is charged to some initial voltage with  $S_1$  and  $S_2$  open (see Fig. 7).  $S_1$  is closed to discharge the capacitor bank. At a predetermined time, the MFCG explosive is detonated; this also closes  $S_2$ . From this time on the capacitor bank is not in the circuit. Current flow is primarily controlled by the generator and rail inductance. In the model, both  $L_G$  and  $L_L$  are calculated as an inductance per unit length ( $L'$ ) of long, parallel conductors multiplied by their length, plus small, constant-inductance contributions. At the start of current flow in the generator or in the rails, both  $L_G$  and  $L_L$  are assumed to be inductances in the high-frequency limit. The calculated inductances have been correlated in terms of

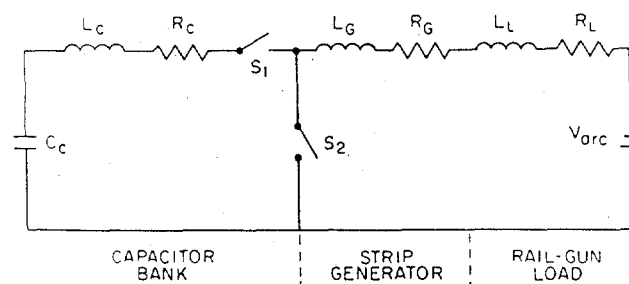


Fig. 7. Lumped parameter circuit model.

conductor size and separation; the correlations are used in this model to reduce computation times. Because the generator conductors are relatively thin,  $L_G$  is assumed to be constant during the calculation. At a given time, the rail inductance gradient ( $L_L$ ) varies along the length of the rails because sections near the breech are in the circuit from the start and current has diffused into the rails, while sections near the muzzle are only in the circuit at later times. A value for  $L_L$  is approximated as an average of the inductance gradient of a sequence of axial rail increments. At each increment, the variation of inductance with current diffusion is estimated from the high-frequency inductance, the steady-state inductance, and a time constant that is a function of rail size. The generator length is modeled as the initial length minus the product of the detonation velocity and burn time. The rail length is taken to be the projectile position plus any section of rails initially in the circuit.

The generator and rail resistances are also calculated as a resistance per unit length of conductor ( $R'$ ) multiplied by the conductor length, plus small, constant-resistance contributions. Values of  $R_G$  and  $R_L$  are assumed to vary between high-frequency limits at the start of current flow and steady-state limits with time constants that depend on conductor size. The high-frequency limits are calculated using penetration depths at  $0.5 \mu s$ .

An arc is used to carry current between the rails behind the projectile. The arc is modeled as a variable voltage ( $V_{arc}$  in Fig. 7) that is a function of total current flow. Data for the arc model were obtained from muzzle voltage measurements on the rails. Muzzle voltages in the 200–700 volt range have been measured with peaks above 1 kV when the projectile leaves the rails.

The model described here has been used to define test conditions for a number of railgun tests. One advantage of the model is that there are no adjustable electrical parameters that must be fit to experimental data. However, it has been necessary to account for friction between the projectile and the railgun barrel. No suitable physical model has been found for friction in this velocity and pressure regime. Most design calculations have been done using an empirical friction model that disregards a constant portion of the accelerating force, normally 20–40%. Figure 8 shows a plot of measured and calculated current at the railgun breech for one test. A 30% friction correction was employed here. The major differences between the calculated and measured curves are in the 450–550  $\mu s$  time range, at the end of the 3-m-long generator burn time. Figure 9 shows a plot of measured and calculated projectile position for this test. The measured positions are from probes located along the rails and at the muzzle of the 1.13-m railgun. The overall agreement between the calculated and measured data is relatively good. Agreement could be improved for the position data (Fig. 9) by using a more complex friction model; however, it would be an ad-hoc model and not appropriate to other tests.

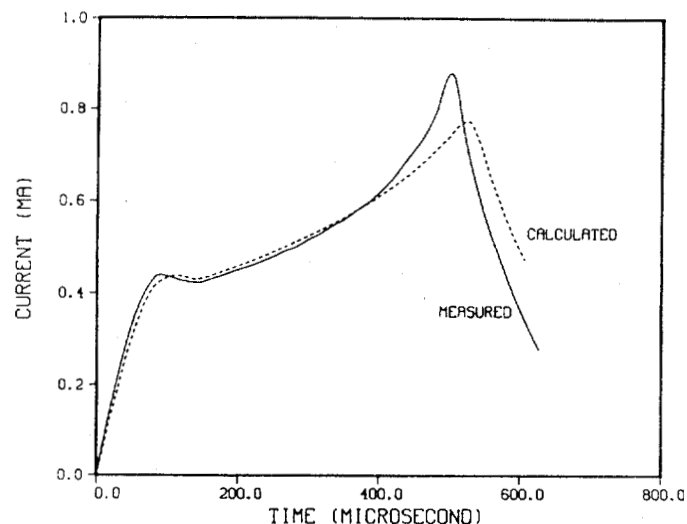


Fig. 8. Rail current as a function of time, October 26, 1982 test.

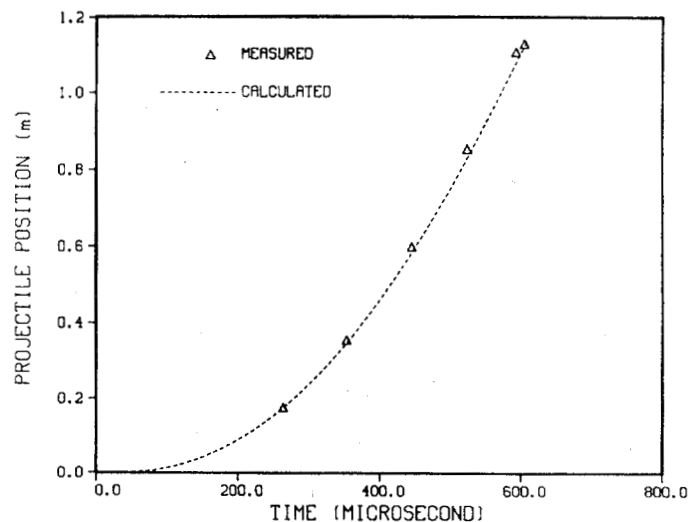


Fig. 9. Projectile position as a function of time, October 26, 1982 test.

#### References

1. J. F. Kerrisk, "Current Distribution and Inductance Calculation for Railgun Conductors," Los Alamos National Laboratory report LA-9092-MS (October 1980).
2. J. F. Kerrisk, "Current Diffusion in Railgun Conductors," Los Alamos National Laboratory report LA-9401-MS (June 1982).
3. C. M. Fowler, D. R. Peterson, J. F. Kerrisk, R. S. Caird, D. J. Erickson, B. L. Freeman, and J. H. Goforth, "Explosive Flux-Compression Generators," presented at the Third International Conference on Megagauss Magnetic Field Generation and Related Topics, June 13–17, 1983, Novosibirsk, USSR.